JOURNAL OF CATALYSIS 126, 546–554 (1990)

The Effect of Sodium on the MoO_3–SiO_2-Catalyzed Partial Oxidation of Methane

NICHOLAS D. SPENCER,* CARMO J. PEREIRA,* AND ROBERT K. GRASSELLI†,‡,[1]

*W.R. Grace & Co. -Conn., Research Division, Columbia, Maryland 21044; †Office of Naval Research, Chemistry Division, Arlington, Virginia 22217; and ‡Department of Chemistry, Georgetown University, Washington, DC 20057

Received January 17, 1990; revised May 7, 1990

The effect of sodium on the partial oxidation of methane over MoO_3–SiO_2 in the presence of molecular oxygen has been investigated. As in the sodium-free case, the major products are formaldehyde, carbon monoxide, carbon dioxide, and water. Kinetic analysis indicates that methane is directly oxidized to formaldehyde and carbon dioxide. Formaldehyde is oxidized to carbon monoxide, which is itself further oxidized, providing an alternative route to carbon dioxide. The kinetic model shows that sodium poisons the direct oxidation of methane to formaldehyde and carbon dioxide, but promotes the oxidation of formaldehyde and carbon monoxide. Model predictions of rates and selectivities are in good agreement with the experimental data. A mechanism that explains both the poisoning and promotion effects of sodium on MoO_3–SiO_2 is proposed.

INTRODUCTION

Alkali metals are ubiquitous in heterogeneous catalysts, and act as both promoters and poisons. While alkalis (generally K) are usually added to iron-based ammonia or Fischer–Tropsch catalysts in order to promote activity (*1, 2*), the presence of potassium in vanadyl pyrophosphate has been found to poison the selective oxidation of *n*-butane to maleic anhydride (*3*), while promoting the pathway to CO_2. Partial oxidation is not universally blocked by the presence of alkali metals, however. In the case of the ammoxidation of olefins over bismuth- and molybdenum-containing systems (*4–7*), the presence of alkali metals improves the selectivity to partial oxidation products (acrylonitrile, acrolein). Recently, MacGiolla Coda and Hodnett (*8*), using MoO_3–SiO_2 with N_2O as an oxidant, reported that sodium poisoned formaldehyde formation from methane at low Mo levels (<0.2 wt% Mo). However, at much higher Mo loadings, sodium was actually found to promote HCHO formation.

We have previously reported (*9–11*) that the partial oxidation of methane to formaldehyde by molecular oxygen is catalyzed by both MoO_3–SiO_2 and V_2O_5–SiO_2. The mechanism over MoO_3–SiO_2 involves the parallel conversion of methane to HCHO and CO_2, with HCHO being further oxidized to CO, the principal oxidation product at high conversions. The V_2O_5–SiO_2 system appears to be a sequential $A \rightarrow B \rightarrow C \rightarrow D$ mechanism, where the CO_2 is formed from the CO. In both cases we noticed that the presence of sodium at even very low concentrations leads to an overall decrease in conversion level and a severe drop in the selectivity to formaldehyde.

In the present paper we present results obtained at various sodium levels in the MoO_3–SiO_2 catalyst and compare them to the corresponding sodium-free data for MoO_3–Cabosil reported in Ref. (*9*). We have also modified a kinetic model previously developed for the sodium-free case

[1] Present address: Mobil Research and Development Corporation, Paulsboro, NJ 08066.

0021-9517/90 $3.00

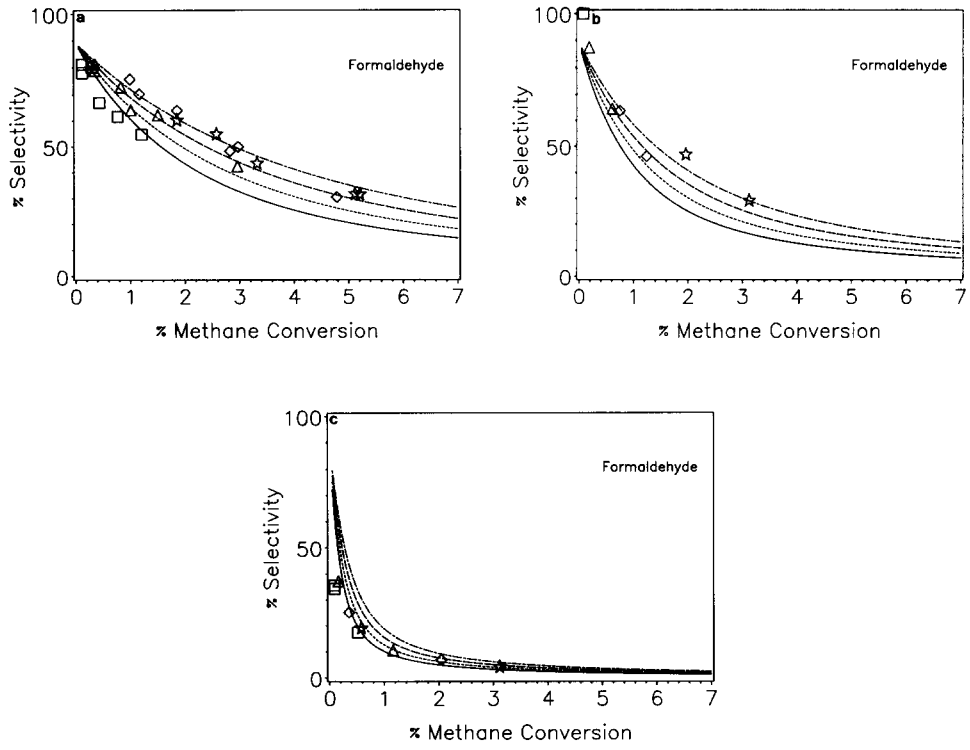

FIG. 1. Formaldehyde selectivity vs methane conversion curves. Symbols correspond to data, lines correspond to model predictions. (□ —— 848 K, △ - - - - 873 K, ◇ ——— 898 K, * - — - — - 923 K); (a) 0 wppm Na, (b) 700 wppm Na, (c) 3600 wppm Na.

(*9*) to account for the conversion and selectivity of methane oxidation over MoO_3–SiO_2 as a function of sodium level. This is not intended to be a rigorous kinetic analysis, but rather an attempt to examine the effect of sodium on the individual reaction steps. Sodium appears to function as both promoter and poison in this system. A key element of the mechanism is the existence of both parallel and sequential CO_2 formation pathways when sodium is present.

EXPERIMENTAL

Catalyst Preparation

All catalysts were prepared starting with Cabosil M5 (a fumed silica manufactured by Cabot Corporation). This was incipient-wetness impregnated with a solution of sodium nitrate, dried at 110°C overnight, and calcined for 2 h at 450°C and 2 h at 600°C in air. This sodium-loaded silica was then incipient-wetness impregnated using ammonium paramolybdate, after which it was dried and calcined once more as described above. The finished powders were compressed at 15,000 psi, crushed, and sieved

TABLE 1

Properties of Catalysts Used in the Present Study

Catalyst	wppm Na	BET surface area ($m^2\ g^{-1}$)
A	0	195
B	319	168
C	700	159
D	900	166
E	1477	156
F	3600	180

Note. All catalysts contain 1.8 wt% Mo as MoO_3.

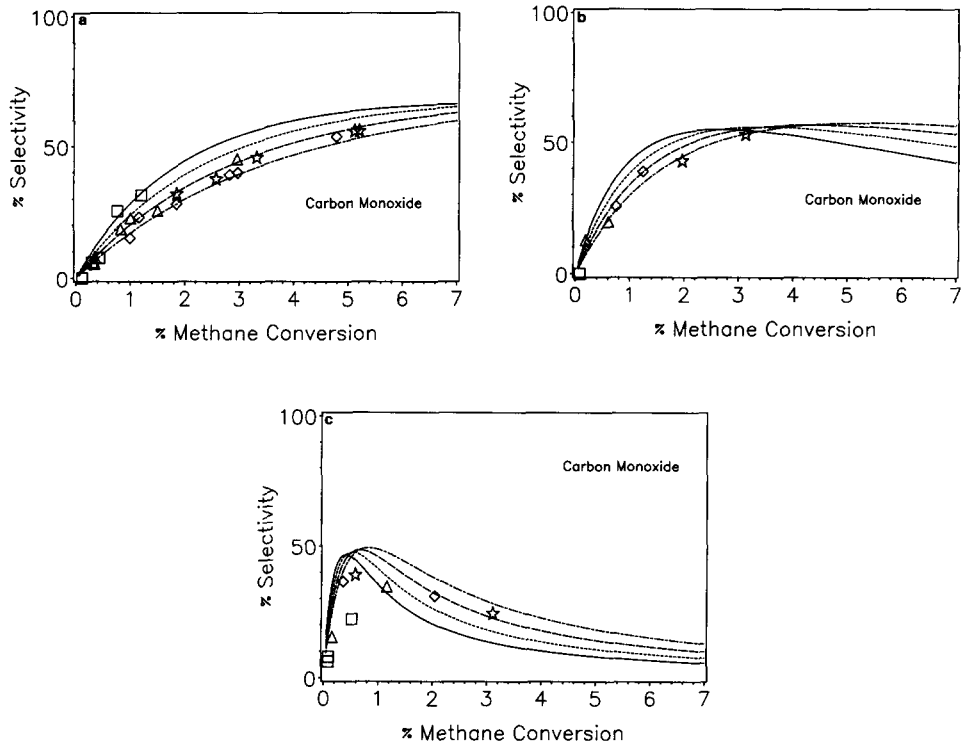

FIG. 2. Carbon monoxide selectivity vs methane conversion curves. Symbols correspond to data, lines correspond to model predictions. (□ —— 848 K, △ - - - - 873 K, ◇ ——— 898 K, * - — - — - 923 K); (a) 0 wppm Na, (b) 700 wppm Na, (c) 3600 wppm Na.

to a particle size of 0.5–0.7 mm. Catalyst properties are summarized in Table 1.

Apparatus and Methods

These have been fully discussed in our previous papers (*9–11*). Catalyst samples of 0.5 cm^3 were loaded into a quartz reactor and covered with an equal volume of quartz chips (which served as a preheating zone.) Experiments were carried out at 1 atm using a mixture containing 10% oxygen and 90% methane, with gas hourly space velocities varying from 2500 to 10,000 h^{-1} (at NTP). The temperature was varied from 848 to 923 K and the effluent analyzed by gas chromatography.

RESULTS

As previously reported (*9, 10*) the primary products of methane oxidation were found to be formaldehyde, carbon monoxide, carbon dioxide, and water. Methanol and hydrogen were only present in trace quantities. Reactor effluent data obtained under varying operating conditions have been plotted in the form of product selectivity (i.e., the percentage of product in the converted methane) vs percentage methane conversion.

Formaldehyde selectivity for 0, 700, and 3600 wppm sodium on catalyst is shown in Figs. 1a, 1b, and 1c, respectively. At a given level of methane conversion, the formaldehyde selectivity was found to decrease with increasing sodium content of the catalyst, and increase with increasing temperature. Also, the temperature dependence of formaldehyde selectivity is reduced with increasing sodium content of the catalyst. At a given sodium level, the formaldehyde selec-

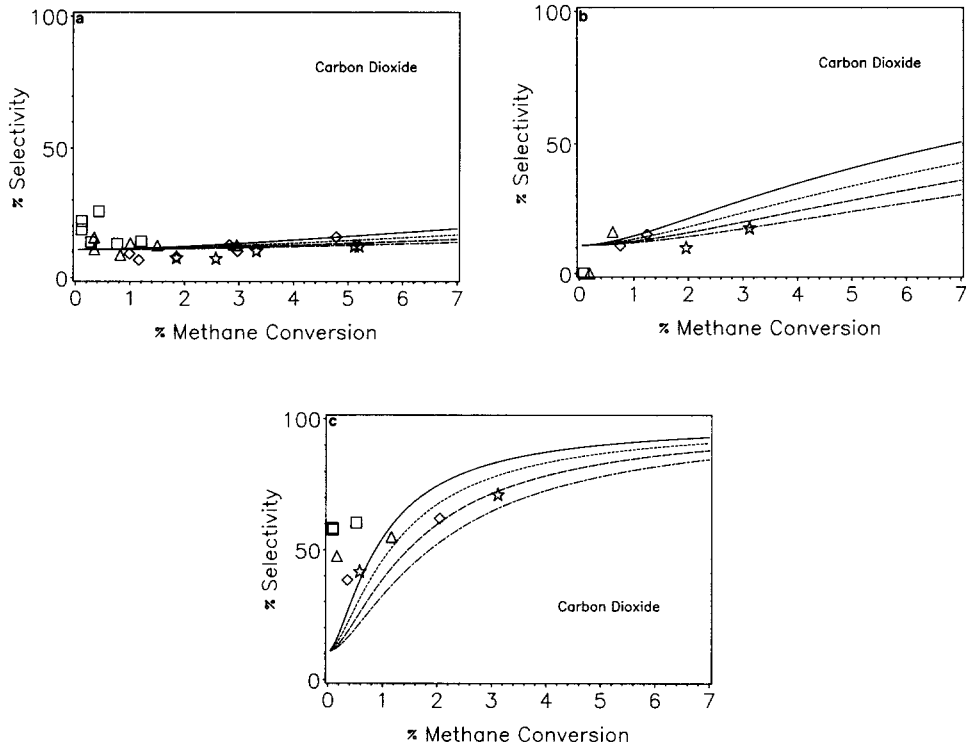

FIG. 3. Carbon dioxide selectivity vs methane conversion curves. Symbols correspond to data, lines correspond to model predictions. (□ —— 848 K, △ - - - - 873 K, ◇ ——— 898 K, * - — - — - 923 K); (a) 0 wppm Na, (b) 700 wppm Na, (c) 3600 wppm Na.

tivity decreases monotonically with increasing methane conversion, indicating that formaldehyde is a primary reaction product.

Carbon monoxide selectivity at the above three sodium levels is shown in Figs. 2a–2c. Selectivity to carbon monoxide tends to zero at zero methane conversion and increases with methane conversion, implying that carbon monoxide is a secondary product. At 3600 wppm sodium loading (*10*) (catalyst F), the carbon monoxide selectivity goes through a maximum, suggesting that the further oxidation of CO is favored at high methane conversions.

Carbon dioxide selectivity for the three sodium levels is shown in Figs. 3a–3c. Selectivity is nonzero at zero methane conversion, implying that carbon dioxide is also a primary product. As discussed in (*9*), carbon dioxide selectivity is fairly constant over a 0 wppm sodium catalyst (A) (Fig. 3a), whereas at the higher sodium levels, carbon dioxide selectivity increases substantially with methane conversion. Scatter at low conversions is due to the practical difficulties of measuring low CO_2 concentrations in the experimental setup described above.

As discussed in (*9–11*), no change in conversion or selectivity behavior was detected when the methane to oxygen ratio was varied provided that oxygen conversion was kept below 100%. This strongly suggests that the reaction is zero order in oxygen.

Based on the above observations, the following reaction scheme may be proposed:

$$CH_4 + O_2 \xrightarrow{k_1} HCHO + H_2O$$

$$HCHO + \tfrac{1}{2}O_2 \xrightarrow{k_2} CO + H_2O$$

$$CH_4 + 2O_2 \xrightarrow{k_3} CO_2 + 2H_2O$$

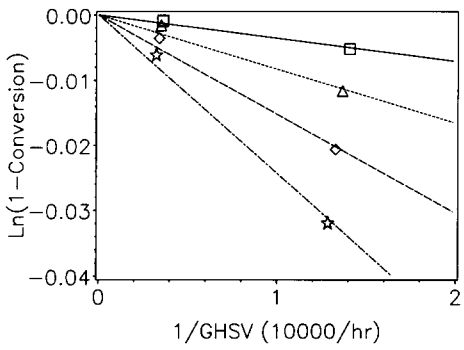

FIG. 4. Rate constant plots based on Eq. (1) for the 3600 wppm Na catalyst (□ 848 K, △ 873 K, ◇ 898 K, * 923 K).

$$CO + \tfrac{1}{2}O_2 \xrightarrow{k_4} CO_2$$

The relationship between the various species and reactor conditions for a reaction that is first order in methane concentration and zero order in oxygen concentration in an isothermal, plug-flow reactor is

$$\ln\left[1 - \left(\frac{c_{HCHO} + c_{CO} + c_{CO_2}}{c^0_{CH_4}}\right)\right] = \frac{-(k_1 + k_3)}{GHSV}, \quad (1)$$

where the left-hand side is simply ln(1-conversion), c is the mole fraction, and GHSV is the gas hourly space velocity at reaction conditions. k_1 and k_3 are the reactor–volume-based rate constants for the CH_4 oxidation reactions.

The left-hand side of Eq. (1) was plotted vs 1/GHSV for each temperature and catalyst sodium level. The resulting straight lines are consistent with methane being oxidized in a first-order reaction (e.g., Fig. 4). The slope of each line corresponds to $-(k_1 + k_3)$ at that particular temperature and sodium level, enabling us to construct a series of Arrhenius plots. $(k_1 + k_3)$ at 923 K is plotted versus sodium content in Fig. 5 and shows that sodium poisons the methane oxidation reaction. The apparent activation energy at all sodium levels was taken to be 189 kJ/mole, the same as was observed for the 0 wppm sodium catalyst (*9*), since there was no apparent trend in activation energies as a function of Na loading. Thus, in the model, the presence of sodium affects only the pre-exponential of the methane decomposition rate constants. The Thiele modulus was calculated at each temperature (*11*) and the methane oxidation reaction was found to be kinetically controlled and not limited by intraparticle diffusion over the temperature range examined. The relative rates of methane oxidation to HCHO and CO_2 are obtained by experimentally determining the ratio $\{(c_{HCHO} + c_{CO})/(c_{HCHO} + c_{CO} + c_{CO_2})\}$ at low conversions when the conversion of CO → CO_2 is negligible. This ratio at low conversions yields $k_1/(k_1 + k_3)$. A $k_1/(k_1 + k_3)$ value of 0.89 was observed at each temperature and for each sodium level. This suggests that the activation energies for the formation of formaldehyde and carbon dioxide are approximately the same and that both k_1 and k_3 are equally poisoned by sodium ($K_1 = K_3$). The solid line in Fig. 5 represents model predictions using rate constant dependences on sodium content of the form

$$k_1 = (k_1^0 e^{-E_1/RT})/(1 + K_1[Na]) \quad (2a)$$

$$k_3 = (k_3^0 e^{-E_3/RT})/(1 + K_3[Na]), \quad (2b)$$

where the values of the rate constant and activation energies are shown in Table 2. A comparison of the predicted methane con-

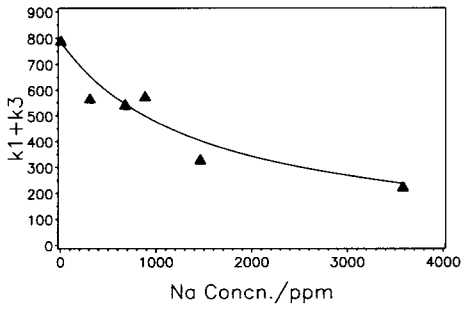

FIG. 5. Effect of sodium content on $(k_1 + k_3)$ at 923 K. Symbols correspond to data, lines correspond to model prediction using Eq. (2).

TABLE 2

Kinetic Parameters

Index	Reaction	k_i (h^{-1}, 873 K) (0 wppm Na)	k_i^0 (h^{-1})	E_i (kJ mol^{-1})	K_i ($wppm^{-1}$)
1	$CH_4 \rightarrow HCHO$	173	2.7×10^{13}	189	0.000648
2	$HCHO \rightarrow CO$	12,800	1.1×10^{12}	134	0.000607
3	$CH_4 \rightarrow CO_2$	21	3.3×10^{12}	189	0.000648
4	$CO \rightarrow CO_2$	542	4.6×10^{9}	117	0.00443

version using Eqs. (1), (2a), and (2b) and the experimental data is shown in Fig. 6. There is good agreement between model and experiment.

A first-order kinetic rate law was used to describe formaldehyde oxidation (*9, 11*). The formaldehyde decomposition rate constant obtained for the 0 wppm sodium case (*8*), however, overpredicted the formaldehyde composition in the reactor effluent. A reasonable fit of the experimental data was obtained when k_2 was modified:

$$k_2 = (1 + K_2[\mathrm{Na}])k_{2,0\,\mathrm{wppm\,Na}}. \quad (3)$$

This suggests that the presence of sodium *promotes* the oxidation of HCHO → CO.

Assuming that the carbon monoxide oxidation proceeds to carbon dioxide via a first-order reaction, an analytical expression for the yield of carbon monoxide was derived. A reasonable fit of the experimental data was obtained when k_4 was modified as

$$k_4 = (1 + K_4[\mathrm{Na}])k_{4,0\,\mathrm{wppm\,Na}}. \quad (4)$$

This suggests that the presence of sodium also promotes the oxidation of CO → CO_2. This expression was used along with a standard nonlinear parameter estimation method to obtain best fit values for k_4^0 and E_4. Values of preexponential factors and activation energies obtained in our study are summarized in Table 2.

Analytical relationships between product selectivities and methane conversion are summarized in Table 3. Selectivities depend on the methane conversion, temperature, and sodium content. Using these selectivity relationships, predicted yields (selectivities × conversions) are compared with the ob-

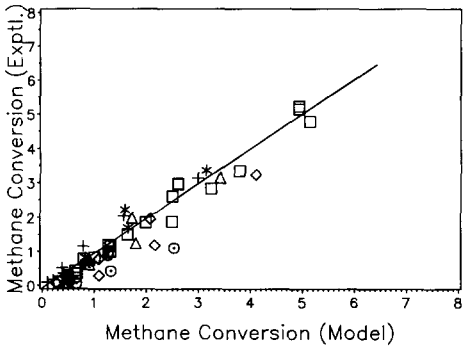

FIG. 6. Comparison of experimental and model-calculated methane conversion. (Na loadings (wppm): □ 0, ◇ 319, △ 700, * 900, ⊙ 1477, and +3600).

TABLE 3

Product Selectivity Expressions for Methane Oxidation via a Sequential Pathway

$$S_{\mathrm{HCHO}} = \frac{k_1}{\{(k_1 + k_3) - k_2\}\Psi}\left[\Psi - 1 + (1 - \Psi)^{k_2/(k_1+k_3)}\right]$$

$$S_{\mathrm{CO}} = \frac{k_1 k_2}{\{(k_1 + k_3) - k_4\}(k_2 - k_4)\Psi}(1 - \Psi)^{k_4/(k_1+k_3)} + \frac{k_1 k_2}{\{k_2 - (k_1 + k_3)\}\Psi}\left[\frac{(1 - \Psi)}{\{k_4 - (k_3 + k_1)\}} - \frac{(1 - \Psi)^{k_2/(k_1+k_3)}}{(k_4 - k_2)}\right]$$

$$S_{\mathrm{CO_2}} = 1 - S_{\mathrm{HCHO}} - S_{\mathrm{CO}}$$

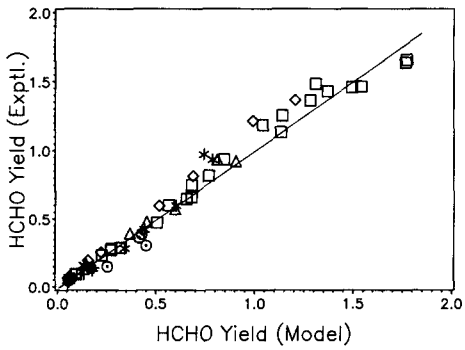

FIG. 7. Comparison of experimental and model-calculated HCHO yield. (Na loadings (wppm): □ 0, ◇ 319, △ 700, * 900, ⊙ 1477, and +3600).

served values for formaldehyde (Fig. 7) and carbon monoxide (Fig. 8). In these figures, the scatter around the "$y = x$" line appears to be due to random error.

The selectivity relationships were also used to draw the lines in Figs. 1–3, which correspond to the model predictions at each temperature. As in the data shown in Fig. 2c, the model predictions of carbon monoxide selectivity show a maximum. Generally, model predictions compare well with the experimental observations.

The mathematical model is built on the assumption that the reaction rate is zero order in oxygen concentration. This assumption should break down when the oxygen concentration becomes very low. This regime was not extensively investigated as the nature of the catalytic surface was thought to change in low oxygen concentrations. The upper limit on the oxygen concentration in the reactant mixture was kept low and well below the explosion limit. The methane conversion was limited by the oxygen present and in no case exceeded 7%. Several of these considerations are similar to those discussed in our previous paper (*9*).

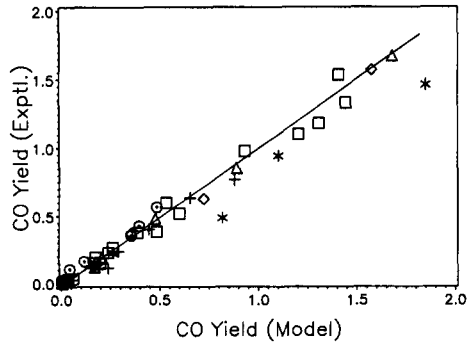

FIG. 8. Comparison of experimental and model-calculated CO yield. (Na loadings (wppm): □ 0, ◇ 319, △ 700, * 900, ⊙ 1477, and +3600).

DISCUSSION

A tentative model for methane partial oxidation, which fits with the behavior described above is shown schematically in Figs. 9 and 10. At the reaction temperatures employed it seems likely that the initial attack on methane is a radical reaction with thermally generated Mo–O· species. The anion vacancies formed in subsequent steps are readily accommodated in the MoO_3 by the formation of shear structures (*12*). After extraction of a hydrogen by an adjacent Mo species, a methoxy intermediate, **1**, is formed. Allison and Goddard (*13*) have discussed the fate of similar intermediates in the methanol oxidation reaction. According to their ab initio GVB calculations, a dual (adjacent) dioxo mechanism leads to the formation of formaldehyde by abstraction of a further hydrogen from the methoxy. Crucial to this mechanism is the formation of partial triple bonds with the "spectator" oxygens. This would clearly be inhibited if sodium were bonded to the oxygen and accounts for the poisoning effect of sodium on this step. The parallel route to CO_2 presumably incorporates the extra C–O bond by the formation of a bridged species, **2** (*14*), and subsequent H-removal by adjacent Mo species. Similar arguments apply to the role of the spectator oxygen and the action of sodium as a poison in this reaction. The methoxy species, **1**, can also pick up a hydrogen from an adjacent hydroxyl group to produce methanol. This does not occur to a great extent in our system.

Further reaction of the HCHO with the

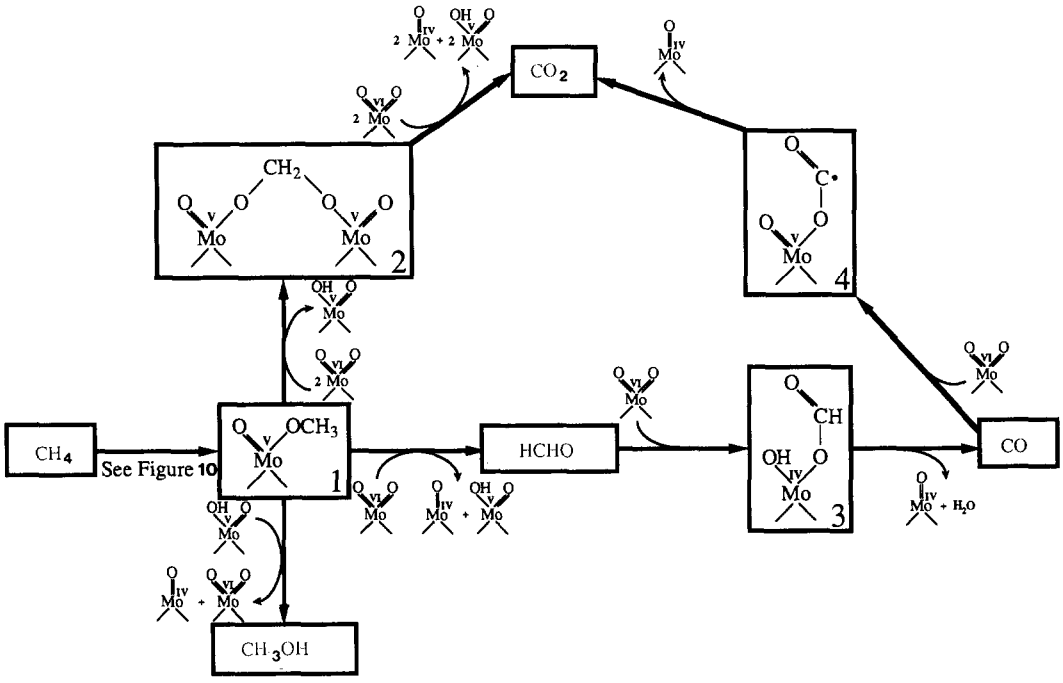

FIG. 9. Reaction pathway schematic for methane oxidation reactions.

surface leads to the formation of the formate species, **3**. This is a well-known intermediate in the water–gas shift reaction, and is known to decompose to CO on acidic catalysts (*15, 16*), including those based on MoO_3. The replacement of one of the =O bonds with —ONa would increase the electron density on the adjacent oxygen, thereby facilitating nucleophilic attack on the formaldehyde. A similar argument can be used in the further reaction of CO with the surface to form a Mo–O–C·–O intermediate, **4** (*14*) which ultimately falls apart to form CO_2.

Thus the action of sodium as both promoter and poison in this system can be explained by the inherently different modes of interaction of the surface with the C–H bonds of CH_4 on the one hand and the C=O bonds of HCHO and CO on the other.

In a previous paper (*10*), we discussed the activity of silica itself for methane partial oxidation to formaldehyde. While silica is approximately an order of magnitude less active for the reaction than MoO_3–SiO_2, it does not appear to be poisoned by the addition of sodium, suggesting that in the MoO_3–SiO_2 system the sodium is primarily

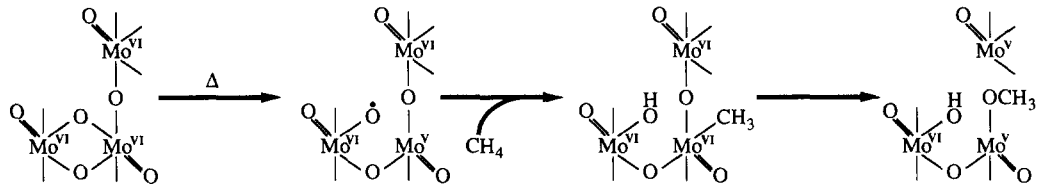

FIG. 10. Reaction pathway schematic for initial attack on methane.

interacting with the Mo-containing species. In the same paper, it was also reported that the active MoO_3, which covers $\approx$0.1 monolayers at our loadings, sublimes far less readily than MoO_3 on silica at higher coverages or bulk MoO_3. This implies a strong interaction between the Mo-containing species and the SiO_2 "support." While the available experimental data do not yet allow us to comment on the precise catalytic roles of this interaction and of the silica itself, the picture that emerges is one of small domains of connected MoO_3 species, pinned in at least one location to the SiO_2, but still able to form shear structures. These low-coverage shear domains would be analogous to the MoO_3 domains that have been proposed in mixed molybdate partial oxidation catalysts (*12*). One function of the sodium in poisoning the initial dehydrogenation reaction (shown in Fig. 10) may be to lock an entire shear domain (*10*) by the formation of an —ONa species which cannot readily be eliminated, thus inhibiting the facile accommodation of anion vacancies. This would account for the dramatic poisoning effect of sodium, even at 300 wppm levels, corresponding to a surface atomic ratio of 1 : 15 : 300, Na : Mo : Si (*10*).

APPENDIX

Notation

c, mole fraction, mol/total mol
c^0, initial mole fraction, mol/total mol
E_i, activation energy, J/mol
GHSV, gas hourly space velocity, m^3 gas/h $\cdot$ m^3 catalyst
k_i, rate constant, h^{-1}
k_i^0, preexponential factor
R, gas constant, J/mol $\cdot$ K
S, selectivity, mole fraction of total oxidized products
Ψ, mole fractional conversion of methane
K_i, activity modification constants defined in text, $wppm^{-1}$

Subscript

i, index

ACKNOWLEDGMENTS

The authors are very grateful to Carole C. Carey for her skillful experimental work and to Dr. Michael J. Wax and Dr. James A. Dumesic for many stimulating discussions.

REFERENCES

1. Mross, W.-D., *Catal. Rev. Sci. Eng.* **25,** 591 (1983).
2. Wesner, D. A., Coenen, F. P., and Bonzel, H. P., *Langmuir* **1,** 478 (1985).
3. Centi, G., Golinelli, G., and Trifiro, F., *Appl. Catal.* **48,** 13 (1989).
4. Grasselli, R. K., Suresh, D. D., and Hardman, H. F., US Pat. 4,778,930 (1988).
5. Grasselli, R. K., and Hardman, H. F., US Pat. 4,767,878 (1988).
6. Grasselli, R. K., and Hardman, H. F., US Pat. 4,503,001 (1985).
7. Grasselli, R. K., and Hardman, H. F., US Pat. 3,642,930 (1972).
8. MacGiolla Coda E., and Hodnett, B. K., "World Congress on Selective Oxidation." Rimini, Italy, 1989.
9. Spencer, N. D., and Pereira, C. J., *AIChE J.* **33,** 1808 (1987).
10. Spencer, N. D., *J. Catal.* **109,** 187 (1988).
11. Spencer, N. D., and Pereira, C.J., *J. Catal.* **116,** 399 (1989).
12. Grasselli, R. K., Burrington, J. D., and Brazdil, J. F., *J. Chem. Soc., Faraday Discuss.* **72,** 203 (1982).
13. Allison, J. N., and Goddard, W. A., *J. Catal.* **92,** 127 (1985).
14. Amiridis, M. D., Rekoske, J. E., Dumesic, J. A., Rudd, D. F., Spencer, N. D., and Pereira, C. J., *AIChE J.*, submitted.
15. Ai, M., *J. Catal.* **50,** 291 (1977).
16. Mars, P., Scholten, J. J. F., and Zwietering, P., *in* "Advances in Catalysis" (D. D. Eley, H. Pines, and P. B. Weisz, Eds.), Vol. 14, p. 35. Academic Press, New York/London, 1963.